Arabidopsis STAYGREEN-LIKE (SGRL) promotes abiotic stress-induced leaf yellowing during vegetative growth

Sakuraba, Yasuhito ; Kim, Dami ; Kim, Ye-Sol ; Hörtensteiner, Stefan ; Paek, Nam-Chon

Abstract: During leaf senescence in Arabidopsis, STAYGREEN 1 (SGR1) and SGR2 regulate chlorophyll degradation positively and negatively, respectively. SGR-LIKE (SGRL) is also expressed in pre-senescing leaves, but its function remains largely unknown. Here we show that under abiotic stress, Arabidopsis plants overexpressing SGRL exhibit early leaf yellowing and sgrl-1 mutants exhibit persistent green color of leaves. Under salt stress, SGR1 and SGRL act synergistically for rapid Chl degradation prior to senescence. Furthermore, SGRL forms homo- and heterodimers with SGR1 and SGR2 in vivo, and interacts with LHCII and chlorophyll catabolic enzymes. The role of SGRL under abiotic stress is discussed.

DOI: https://doi.org/10.1016/j.febslet.2014.09.018

Title Page

Running title: SGR-LIKE promotes stress-induced leaf yellowing

Arabidopsis STAYGREEN-LIKE (SGRL) promotes abiotic stress-induced leaf yellowing during vegetative growth

Yasuhito Sakuraba[1]*, Dami Kim[1], Ye-Sol Kim[1,2], Stefan Hörtensteiner[3], and Nam-Chon Paek[1]*

[1] Department of Plant Science, Plant Genomics and Breeding Institute, Research Institute of Agriculture and Life Sciences, Seoul National University, Seoul 151-921, Korea
[2] Present address: Advanced Radiation Technology Institute, Korea Atomic Energy Research Institute, Jeongeup 580-185, Korea
[3] Institute of Plant Biology, University of Zurich, CH-8008 Zurich, Switzerland
*Corresponding authors: E-mail, sakuraba0425@gmail.com or ncpaek@snu.ac.kr; Tel, + 82 2 8804543; Fax, +82 2 8774550

Keywords: Chlorophyll degradation; STAYGREEN (SGR); SGR-LIKE (SGRL); SGRL-CCE-LHCII interaction; abiotic stress.

Abbreviations

CBB, Coomassie Brilliant Blue; Chl, chlorophyll; CCE, chlorophyll catabolic enzyme; *CLH*, *CHLOROPHYLLASE*; DDI, days of dark incubation; DST, days of salt treatment; GFP, green fluorescent protein; LHCI, light-harvesting complex I; LHCII, light-harvesting complex II; *NYC1*, *NON-YELLOW COLORING 1* (At4g13250); *NOL*, *NYC1-LIKE* (At5g04900); *HCAR*, 7-*HYDROXYMETHYL CHLOROPHYLL A REDUCTASE* (At1g04620); MCS, metal-chelating substance; *PPH*, *PHEOPHYTINASE* (At5g13800); *PAO*, *PHEOPHORBIDE A OXYGENASE* (AT3G44880); *RCCR*, *RED CHLOROPHYLL CATABOLITE REDUCTASE* (AT4G37000); *SGR1/NYE1*, *STAYGREEN 1/NONYELLOWING 1* (At4g22920); *SGRL*, *SGR-LIKE* (At1g44000).

Abstract

During leaf senescence in *Arabidopsis*, *STAYGREEN 1* (*SGR1*) and *SGR2* regulate chlorophyll degradation positively and negatively, respectively. *SGR-LIKE* (*SGRL*) is also expressed in pre-senescing leaves, but its function remains largely unknown. Here we show that under abiotic stress, *Arabidopsis* plants overexpressing *SGRL* exhibit early leaf yellowing and *sgrl-1* mutants exhibit persistent green color of leaves. Under salt stress, *SGR1* and *SGRL* act synergistically for rapid Chl degradation prior to senescence. Furthermore, SGRL forms homo- and heterodimers with SGR1 and SGR2 *in vivo*, and interacts with LHCII and chlorophyll catabolic enzymes. The role of SGRL under abiotic stresses is discussed.

1. Introduction

Chlorophyll (Chl) harvests light and transfers excitation energy (or electrons) to other components of the photosynthetic electron transport chain within chloroplasts of leaves before senescence [1]. However, free Chl and several of its breakdown intermediates are phototoxic; therefore, in the gerontoplasts of senescing leaves, Chl must be degraded along with proteins and other macromolecules [2, 3]. During leaf senescence, Chl is eventually converted to non-phototoxic colorless catabolites, termed phyllobilins, through the PAO/phyllobilin pathway [4], comprising consecutive reactions catalyzed by Chl catabolic enzymes (CCEs) in chloroplasts [5, 6]. To date, six CCE genes, *NON-YELLOW COLORING 1* (*NYC1*) [7, 8], *NYC1-LIKE* (NOL) [8], *7-HYDROXYMETHYL CHLOROPHYLL REDUCTASE* (*HCAR*) [9], *PHEOPHYTINASE* (*PPH*) [10], *PHEOPHORBIDE A OXYGENASE* (*PAO*) [2], and *RED CHLOROPHYLL CATABOLITE REDUCTASE* (*RCCR*) [3], have been identified and characterized in rice (*Oryza sativa*) and *Arabidopsis*. Although PPH is considered as the main dephytylating enzyme in Chl breakdown reactions in *Arabidopsis* leaves [10], chlorophyllase (CLH) is also considered to function as one of the CCEs. The *Arabidopsis CLH1* is induced by wounding or pathogen attack [11, 12], and the CLH1-RNAi lines showed a strong tolerance phenotype to pathogen infection [12], indicating that CLH1 plays an important role in the stress-induced Chl degradation. Although CLH1 and CLH2 in *Arabidopsis* do not localize to chloroplasts [13], citrus CLH functions as a rate-limiting CCE for Chl degradation in the chloroplasts [14], indicating that the contribution of CLH isoforms to Chl catabolism differs between plant species. Furthermore, the metal-chelating substance (MCS) responsible for Mg removal remains unidentified [15].

In addition to CCEs, *STAYGREEN* (*SGR*) functions as a key regulator of Chl degradation. Mutations in *SGR* orthologs cause a stay-green phenotype in many plant species, including *Arabidopsis* (termed *NONYELLOWING 1* [*NYE1*]) [16], rice [17], pea (*Pisum sativum*) [18], tomato (*Solanum lycopersicum*) and bell pepper (*Capsicum annuum*) [19], tall fescue (*Festuca arundinacea*) [20], *Medicago truncatula* [21], and soybean (*Glycine max*) [22]. SGR1/NYE1 physically interacts with light-harvesting complex subunits of photosystem II (LHCII) and six CCEs (NYC1, NOL, HCAR, PPH, PAO, and RCCR), and forms a multi-protein complex for Chl detoxification during leaf senescence [23, 24]. Furthermore, *Solanum lycopersicum* SGR1

(SlSGR1) physically interacts with one of the carotenoid biosynthetic enzymes, phytoene synthase 1 (PSY1), and regulates accumulation of carotenoids, such as lycopene and β-carotene [25].

Chl degradation occurs during leaf senescence, and under biotic/abiotic stress conditions. SGR1 is required for stress-induced leaf yellowing; *noc1*, a mutant allele of *Arabidopsis SGR1*, showed delayed disease symptoms in response to infection of a fungal pathogen [26]. Furthermore, *nye1-1* mutants exhibited a stay-green phenotype under abiotic stress conditions, including high salinity, drought, heat, and high light stresses [27, 28], indicating that SGR1 has an important role in Chl degradation in pre-senescing leaves under abiotic stress. However, compared to senescent leaves, during vegetative growth, leaves have much lower *SGR1* transcript levels [28]. Thus, it is unclear whether SGR1 plays a central role in stress-induced Chl degradation before senescence.

Higher plants have two or more *SGR* homologs, all of which are predicted to localize to the chloroplast [19], indicating that they also may function in Chl metabolism. *Arabidopsis thaliana* has three *SGR* homologs, *SGR1*, *SGR2*, and *SGR-LIKE* (*SGRL*) [19]. We recently reported that *Arabidopsis* plants overexpressing *SGR2* stayed green much longer than wild type plants; also, plants containing *sgr2-1*, a knockout mutant allele of *SGR2*, exhibited early leaf yellowing under age-, dark-, and stress-induced senescence, indicating that SGR2 negatively regulates Chl degradation [28]. By contrast, it appears that SGRL activity is limited to pre-senescing leaves because its expression is rapidly down-regulated in senescing leaves [28]. On the protein level, SGRL is highly similar to SGR1 and SGR2 except for the C-terminal region, and, notably, all photosynthetic plants contain a single copy of *SGRL* [19, 28]. Rong et al. (2013) recently reported that transgenic rice plants overexpressing *OsSGRL* exhibit early leaf yellowing during dark-induced senescence [29], strongly suggesting that SGRL also has an important role in Chl degradation, at least in rice.

In this study, we show that *SGRL*-overexpressing (*SGRL*-OX) plants in *Arabidopsis* exhibit early leaf yellowing under different abiotic stress conditions. Also, *sgrl-1* knockout mutants show a stay-green phenotype under salt stress, an effect that became much stronger in the *nye1-1* mutant background. We demonstrate that SGRL interacts with LHCII subunits and CCEs at the thylakoid membranes *in vivo*. Furthermore, SGRL forms homodimers or heterodimers with SGR1 and SGR2, and it appears that this dimerization is important for the regulation of SGRL activity. Thus, we propose that SGRL mainly contributes to abiotic stress-induced leaf yellowing during vegetative plant growth.

2. Materials and methods

2.1. Plant materials and growth conditions

Arabidopsis thaliana ecotype Columbia-0 (Col-0) was used as wild type. The T-DNA insertion mutant *sgrl-1* (SALK_084849) was obtained from the Arabidopsis Biological Resource Center (ABRC, USA). Plants were grown on soil in a growth chamber at 22-24°C under cool-white fluorescent light (90-100 μmol m^{-2} s^{-1}) under long-day (LD; 16 h light/8 h dark) conditions. For dark treatment of whole plants, 3-week-old plants were transferred to complete darkness. After dark incubation, the rosette leaves were sampled under safe green light. Analyses of salt, osmotic, ABA-induced and drought stresses was performed as previously described [27, 28].

2.2. Plasmid construction and Arabidopsis transformation

The full-length cDNAs of *Arabidopsis SGRL* (At1g44000), rice *OsSGR* (Os09g36200), and *OsSGRL* (Os04g59610) with or without stop codons were amplified by RT-PCR. After insertion into the Gateway entry vector pCR8/GW/TOPO (Invitrogen), the cDNA inserts were recombined into the binary Gateway vectors, pMDC85, pEarleyGate 202 and 205, for expressing the C-terminal GFP, FLAG, and TAP fusion tags, respectively, or pMDC32 for expressing the tag-free native SGRL protein [30]. The primers used for cloning are listed in Supplemental Table 1. *Arabidopsis* transgenic plants were generated by *Agrobacterium tumefaciens* (strain GV3101)-mediated transformation by a floral dipping method [31]. Homozygous T_2 lines were identified on selective agar plates and their progenies used in this study. As a negative control for *in vivo* pull-down assays, transgenic plants carrying *P35S:GFP* were used [23].

2.3. Pigment analysis

Total Chl was extracted from the 2nd or 3rd rosette leaves using ice-cold acetone at 4°C. Supernatants were diluted with ice-cold water to a final acetone concentration of 80%. Chl was quantified spectrophotometrically as previously described [32].

2.4. SDS–PAGE and immunoblot analysis

SDS-PAGE and immunoblot analysis were performed as previously described [28]. For visualization of protein bands, polyacrylamide gels were stained with Coomassie Brilliant Blue

(CBB; Sigma–Aldrich). Antibodies against GFP (Abcam), SGR [17], NYC1 and NOL [8], PAO (Agrisera, Sweden), RCCR [3], and photosystem proteins (Agrisera, Sweden) were used for immunoblot analysis.

2.5. Laser Scanning Confocal Microscopy

GFP fluorescence images were recorded with a laser scanning confocal microscope (LSM510, Zeiss). An argon laser (25 mW) was used to generate an excitation source at 488 nm. GFP and Chl fluorescence were recorded at 525 nm and 660 nm, respectively.

2.6. In vitro and in vivo pull-down assays

For analysis of *in vivo* interactions between SGRL and CCEs, total proteins were extracted from the leaves of 3-week-old plants (3 DDI), and membrane-enriched fractions were purified using the Native Membrane Protein Extraction Kit (Calbiochem). Protein extracts were adjusted based on Chl concentration. To examine the interactions between SGRL and the two SGR proteins (SGR1 and SGR2) by *in vitro* pull-down assays, one-week-old etiolated seedlings were used for protein extraction. Protein extracts were adjusted based on total protein concentration, and anti-GFP antibody-conjugated agarose beads (MBL, Japan) were used for pull-down experiments as described previously [23]. The beads were washed at least three times with washing buffer (50 mM Tris-HCl [pH 7.2], 200 mM NaCl, 0.1% [v/v] Nonidet P-40, 2 mM EDTA, and 10% [v/v] glycerol). Washed beads were boiled with 20 μL of sample buffer for 5 min and then subjected to SDS-PAGE and immunoblot analysis.

2.7. Yeast two-hybrid assays

The full-length *SGRL* cDNA in the entry vector pCR8/GW/TOPO was inserted into the destination vector pDEST32 (bait) (Invitrogen). Prey vectors for six *CCE*s were previously prepared in pDEST22 [23, 24]. The yeast strain MaV203 was used for co-transformation of bait and prey clones, and β-galactosidase activity was measured by a liquid assay using chlorophenol red-β-D-galactoside (CPRG; Roche Applied Science) according to the Yeast Protocol Handbook (Clontech).

2.8. Gene expression analysis by qRT-PCR

The qRT-PCR analyses were performed as previously reported [28]. The transcript levels of each gene were normalized to those of *GAPDH* (glyceraldehyde phosphate dehydrogenase, At1g16300) in *Arabidopsis*. The primers used in qRT-PCR are listed in Supplemental Table 1.

3. Results and discussion

We previously showed that *SGRL* transcripts are abundant in leaves during vegetative growth and decrease in senescing leaves [28]. Thus, *SGRL* expression has a pattern opposite to that of *SGR1* and *SGR2*, which are highly induced only during leaf senescence [26]. Based on this pattern, we assumed that SGRL is not required for Chl breakdown during leaf senescence, but may have an important role in Chl catabolism and/or Chl turnover in leaves during vegetative stages [33].

To investigate the possible roles of *Arabidopsis* SGRL, we produced *Arabidopsis* plants containing a *P35S:SGRL-GFP* transgene (hereafter *SGRL*-OX; see Methods). The expression levels of *SGRL-GFP* in four independent lines were evaluated by qRT-PCR and a line (#4) showing the highest expression was used in this study (Fig. 1A). First, we checked the *SGRL*-OX phenotype under salt stress (200 mM NaCl). At 4 days of salt treatment (DST), *SGRL*-OX plants exhibited early leaf yellowing, similar to *SGR1*-OX (*P35S:SGR1-GFP*) plants, as reported previously [22] (Fig. 1B). Similarly, early leaf yellowing occurred in the detached leaves of *SGRL*-OX (Fig. 1C, D). Consistent with the Chl levels, photosystem proteins (Lhcb1, D1, and Lhca1) were also drastically decreased in *SGRL*-OX (Fig. 1E). Furthermore, ion leakage rates, an indicator of membrane disintegration and cell death, were much higher in *SGRL*-OX under salt stress (Fig. 1F). Notably, leaf color and Chl content of *SGRL*-OX leaves at the vegetative stage were similar to WT (Fig. 1C, D), as well as to *SGR1*-OX [23]. This probably is related to the expression of CCEs, which remain low under non-stress conditions but increase significantly under salt stress conditions (Supplemental Fig. 1). We also found that *SGRL*-OX showed early leaf yellowing under other abiotic stresses, such as osmotic (Supplemental Fig. 2), ABA-induced (Supplemental Fig. 3), and drought stresses (Supplemental Fig. 4), quite similar to *SGR1*-OX [28]. Furthermore, we prepared other *SGRL*-overexpressing lines, including *P35S:SGRL* (non-tagged) and *P35S:SGRL-FLAG*. These overexpressors also showed an early leaf yellowing phenotype under salt stress conditions (Supplemental Fig. 5). These results indicate that SGR1 and SGRL play important roles in abiotic stress-induced leaf yellowing. Under dark-induced senescence (DIS) conditions,

however, leaf yellowing in *SGRL*-OX was much slower than in *SGR1*-OX, but it started slightly earlier than wild type (WT) (Supplemental Fig. 6), suggesting that the contribution of SGRL to dark-induced Chl degradation is relatively small compared to stress-induced Chl breakdown.

Unlike *Arabidopsis*, rice contains only two *SGR*s, *OsSGR* and *OsSGRL*. Mutation of *OsSGR* (Os09g36200) caused a nonfunctional stay-green phenotype in rice during natural senescence and DIS [17], and *OsSGRL*-OX (Os04g59610) showed leaf yellowing even in developing leaves, similar to *OsSGR*-OX [17, 29], indicating that both OsSGR and OsSGRL are positive regulators of Chl degradation in rice. To examine whether stress-induced leaf yellowing also requires OsSGR and/or OsSGRL, we developed *Arabidopsis OsSGR*-OX (*P35S:OsSGR-GFP*) and *OsSGRL*-OX (*P35S:OsSGRL-GFP*) plants. Expression levels of *OsSGR* and *OsSGRL* in four independent lines were evaluated by qRT-PCR (Fig. 2A and 2B). Under normal growth conditions, leaf color of both *OsSGR*-OX and *OsSGRL*-OX was similar to WT (Fig. 2C), dissimilar to the leaf yellowing phenotype caused by overexpressing *OsSGR* and *OsSGRL* in rice [16, 28]. At 3 DST, we found that degreening of *OsSGR*-OX and *OsSGRL*-OX *Arabidopsis* leaves was much faster than that of WT leaves (Fig. 2C), with lower Chl levels (Fig. 2D) and higher ion leakage rates (Fig. 2E), similar to the *Arabidopsis SGR1*-OX and *SGRL*-OX leaves (Fig. 1). Thus, we concluded that the biochemical functions of rice SGR and SGRL correspond to those of *Arabidopsis* SGR1 and SGRL, at least under abiotic stress conditions.

To analyze the effect of *SGRL* deficiency on Chl breakdown in *Arabidopsis*, we isolated a T-DNA insertion mutant of *SGRL* (*sgrl-1*, SALK_084849) (Fig. 3A). The absence of *SGRL* transcripts in *sgrl-1* was confirmed by RT-PCR, indicating that *sgrl-1* is a knockout line (Fig. 3B). Like *SGRL*-OX, *sgrl-1* grew normally and did not show any defects throughout development (data not shown). At 5 DST, however, *sgrl-1* showed a weak stay-green phenotype similar to *nye1-1* [16] (Fig. 3C). Consistent with the visible phenotype, total Chl levels were higher (Fig. 3D) and ion leakage rates were lower in *sgrl-1* (Fig. 3E). To confirm the specificity of the effect of the T-DNA insertion in *sgrl-1*, a complementation test was performed. The conditional stay-green phenotype of *sgrl-1* leaves was recovered by introduction of *35S:SGRL* (Supplemental Fig. 7). Interestingly, the effect of *nye1-1* and *sgrl-1* mutations on salt stress-induced Chl degradation was additive because Chl retention in *nye1-1 sgrl-1* leaves was substantially higher than in either single mutant (Fig. 3C), indicating that *Arabidopsis* SGR1 and SGRL act additively in stress-induced leaf yellowing.

We previously showed that *Arabidopsis* SGR1 and SGR2 localize to the thylakoid membrane of chloroplasts and interact with LHCII [23, 28]. We examined the localization of SGRL-GFP by laser scanning confocal microscopy. In *SGRL*-OX (*P35S:SGRL-GFP*) plants, GFP fluorescence overlapped with the red Chl fluorescence within chloroplasts (Fig. 4A). In addition, SGRL-GFP was mostly detected in membrane-enriched protein fractions extracted from mature leaves (Fig. 4B), indicating that SGRL also localizes to the thylakoid membrane. We subsequently used *in vivo* pull-down assays to examine whether SGRL also interacts with LHCII. Indeed, SGRL co-immunoprecipitated LHCII subunits (Lhcb1, Lhcb2 and Lhcb4), but not with other photosystem subunits such as CP43, Lhca1, and Lhca2 (Fig. 4C), indicating that SGRL also binds specifically to LHCII. Pairwise examination of interactions between SGRL and six CCEs by yeast two-hybrid (Y2H) assays revealed that SGRL strongly interacts with NOL, HCAR, and RCCR, which are abundant in greening seedlings and pre-senescing leaves [24] (Fig. 4D). By contrast, interaction of SGRL with senescence-induced CCEs (NYC1, PPH, and PAO) was relatively weak compared with their interaction with SGR1 [28]. To confirm the Y2H assay results, we performed *in vivo* pull-down assays using 4 anti-CCE antibodies (note that antibodies against HCAR and PPH are currently unavailable and that the anti-SGR antibody detects both SGR1 and SGR2) (Fig. 4E). Because protein levels of NYC1, PAO, and SGR1 were low under salt stress compared with DIS (Supplemental Fig. 8), we incubated *SGRL*-OX plants in darkness for 2 days before performing pull-down assays. Under these conditions, SGRL interacted with all four tested CCEs (Fig. 4E). These results indicate that, like SGR1, ectopically expressed SGRL can form a dynamic complex with CCEs and LHCII in gerontoplasts [22]. We also found that SGRL can form homo- or heterodimers with SGR1 and SGR2 (Fig. 5), similar to SGR1 and SGR2 [28]. It can be assumed that dimer formation is also important for the regulation of SGRL activity.

We subsequently measured the expression of *SGR1* and *SGRL* under salt (150 mM NaCl) and osmotic (400 mM mannitol) stress conditions. Under both conditions, *SGR1* expression increased until 3 h of treatment (HT) and then decreased thereafter (Fig. 6A and 6B). By contrast, *SGRL* expression gradually decreased after 1 or 2 HT (Fig. 6C and 6D). Notably, the increase of *SGR1* expression under these abiotic stresses was less strong than that observed during DIS or natural senescence (Supplemental Fig. 9). Furthermore, the *SGRL* mRNA was much more abundant than the *SGR1* mRNA at the vegetative stage [28] (Fig. 6**)**. Together, these results imply an important role for SGRL, mainly in the early phase of stress-induced Chl degradation in *Arabidopsis*. To

examine the transcriptional relationship between *SGR1* and *SGRL*, we further measured the mRNA levels of *SGR1* in *sgrl-1* mutants and the mRNA levels of *SGRL* in *nye1-1* mutants under salt and mannitol stress conditions, but their levels were not significantly altered (Supplemental Fig. 10), indicating that *SGR1* and *SGRL* expression are regulated independently of each other. This may explain the additive stay-green phenotype in *sgrl-1 nye1-1* mutants.

In this study, we show that abiotic stress-induced leaf yellowing involves SGRL in addition to SGR1; also, SGRL strongly interacts with three CCEs (NOL, HCAR, and RCCR) and LHCII (Fig. 4). It is noteworthy that *nye1-1 sgrl-1* double mutants showed an additive stay-green phenotype (Fig. 3), strongly suggesting that SGR1 and SGRL act synergistically for rapid Chl degradation in pre-senescing leaves. Thus, it appears that in addition to an SGR1-CCE-LHCII complex [23], SGRL can form a similar complex with three CCEs at LHCII in pre-senescing leaves under abiotic stress conditions, which possibly accelerates metabolic channeling of Chl breakdown intermediates to avoid accidental release of phototoxic Chl and Chl catabolites.

During natural senescence, differences of leaf yellowing rates between *SGRL*-OX and WT are hardly distinguishable (data not shown); however, we consistently observed that *SGRL*-OX lines started leaf yellowing slightly earlier than WT, but their leaf yellowing progressed more slowly than *SGR1*-OX leaves during DIS (Supplemental Fig. 6). This discrepancy between the phenotypes of *SGR1*-OX and *SGRL*-OX during DIS is not fully understood; it may be due to protein domain differences in the C-terminal region between SGR1 and SGRL. Sequence analysis of SGR and SGRL proteins from higher plants revealed that the C-terminal region of SGR subfamily members contains a cysteine-rich motif that is absent in the SGRL subfamily. This motif could be involved in redox control [5]; thus, one could speculate that during DIS, SGR1 and SGR2 are redox-regulated, but SGRL cannot be activated by this means. This needs to be further investigated in the future, e.g. by domain swapping experiments of the C-terminal regions of SGR1 and SGRL. The other intriguing matter is the involvement of CLH1 in the stress-induced Chl degradation. During pathogen infection, Arabidopsis CLH1-RNAi plants showed a tolerant phenotype [12], similar to *noc1*, one of the mutant alleles of *SGR1* [26]. Thus, it is possible that, at least under stress conditions, CLH1 is directly involved in the Chl degradation, probably together with SGR1, SGRL, or CCEs. Further biochemical studies are necessary for revealing their functional relationship in leaf yellowing under abiotic/biotic stresses.

Acknowledgments

We are most grateful to Dr. Ayumi Tanaka for providing antibodies against NOL and NYC1, and Dr. Benke Kuai for donating *nye1-1* seeds. This work was carried out with the support of "Cooperative Research Program for Agriculture Science & Technology Development (PJ00812802)", Rural Development Administration, Republic of Korea (N.-C.P.), and by grants of the Swiss National Science Foundation (S.H).

References

[1] Grossman, A. R., Bhaya, D., Apt, K. E. & Kehoe, D. M. (1995) Light-harvesting complexes in oxygenic photosynthesis: diversity, control, and evolution, Ann. Rev. Genet. **29**, 231-88.

[2] Pružinská, A., Tanner, G., Anders, I., Roca, M. & Hörtensteiner, S. (2003) Chlorophyll breakdown: pheophorbide a oxygenase is a Rieske-type iron-sulfur protein, encoded by the accelerated cell death 1 gene, Proc. Natl. Acad. Sci. USA 100, 15259-64.

[3] Pružinská, A., Anders, I., Aubry, S., Schenk, N., Tapernoux-Luthi, E., Müller, T., Kräutler, B. & Hörtensteiner, S. (2007) In vivo participation of red chlorophyll catabolite reductase in chlorophyll breakdown, Plant Cell 19, 369-87.

[4] Kräutler, B. and Hörtensteiner, S. (2013) Chlorophyll breakdown: chemistry, biochemistry and biology. In Handbook of Porphyrin Science (Ferreira, G.C., Kadish, K.M., Smith, K.M. and Guilard, R., eds), pp. 117-185. World Scientific Publishing, Hackensack, NJ, USA.

[5] Hörtensteiner, S. (2009) Stay-green regulates chlorophyll and chlorophyll-binding protein degradation during senescence, Trends Plant Sci. 14, 155-62.

[6] Hörtensteiner, S. (2006) Chlorophyll degradation during senescence, Annu. Rev. Plant Biol. 57, 55-77.

[7] Kusaba, M., Ito, H., Morita, R., Iida, S., Sato, Y., Fujimoto, M., Kawasaki, S., Tanaka, R., Hirochika, H., Nishimura, M. & Tanaka, A. (2007) Rice NON-YELLOW COLORING1 is involved in light-harvesting complex II and grana degradation during leaf senescence, Plant Cell 19, 1362-75.

[8] Horie, Y., Ito, H., Kusaba, M., Tanaka, R. & Tanaka, A. (2009) Participation of chlorophyll *b* reductase in the initial step of the degradation of light-harvesting chlorophyll *a*/*b*-protein complexes in Arabidopsis, J. Biol. Chem. 284, 17449-56.

[9] Meguro, M., Ito, H., Takabayashi, A., Tanaka, R. & Tanaka, A. (2011) Identification of the 7-hydroxymethyl chlorophyll a reductase of the chlorophyll cycle in Arabidopsis, Plant Cell 23, 3442-53.

[10] Schelbert, S., Aubry, S., Burla, B., Agne, B., Kessler, F., Krupinska, K. & Hörtensteiner, S. (2009) Pheophytin pheophorbide hydrolase (pheophytinase) is involved in chlorophyll breakdown during leaf senescence in Arabidopsis, Plant Cell 21, 767-85.

[11] Benedetti, C.E., Costa, C.L., Turcinelli, S.R., and Arruda, P. (1998) Differential expression of a novel gene in response to coronatine, methyl jasmonate, and wounding in the Coi1 mutant of Arabidopsis, Plant Physiol. 116, 1037-42.

[12] Kariola, T, Brader, G, Li, J., and Palva, E.T. (2005) Chlorophyllase 1, a damage control enzyme, affects the balance between defense pathways in plants, Plant Cell 17, 282-94.

[13] Schenk, N., Schelbert, S., Kanwischer, M., Goldschmidt, E.E., Dörmann, P. & Hörtensteiner, S. (2007) The chlorophyllases AtCLH1 and AtCLH2 are not essential for senescence-related chlorophyll breakdown in *Arabidopsis thaliana*, FEBS Lett. 581, 5517-25.

[14] Harpaz-Saad, S., Azoulay, T., Arazi, T., Ben-Yaakov, E., Mett, A., Shiboleth, Y.M., Hörtensteiner, S., Gidoni, D., Gal-On, A., Goldschmidt, E.E. & Eyal, Y. (2007) Chlorophyllase is a rate-limiting enzyme in chlorophyll catabolism and is posttranslationally regulated, Plant Cell 19, 1007-22.

[15] Hörtensteiner, S. (2013) Update on the biochemistry of chlorophyll breakdown, Plant Mol. Biol. 82, 505-17.

[16] Ren, G., An, K., Liao, Y., Zhou, X., Cao, Y., Zhao, H., Ge, X. & Kuai, B. (2007) Identification of a novel chloroplast protein AtNYE1 regulating chlorophyll degradation during leaf senescence in Arabidopsis, Plant Physiol. 144, 1429-41.

[17] Park, S.-Y., Yu, J.-W., Park, J.-S., Li, J., Yoo, S.-C., Lee, N.-Y., Lee, S.-K., Jeong, S.-W., Seo, H. S., Koh, H.-J., Jeon, J.-S., Park, Y.-I. & Paek, N.-C. (2007) The senescence-induced staygreen protein regulates chlorophyll degradation, Plant Cell 19, 1649-64.

[18] Sato, Y., Morita, R., Nishimura, M., Yamaguchi, H. & Kusaba, M. (2007) Mendel's green cotyledon gene encodes a positive regulator of the chlorophyll-degrading pathway, Proc. Natl. Acad. Sci. USA 104, 14169-74.

[19] Barry, C. S., McQuinn, R. P., Chung, M. Y., Besuden, A. & Giovannoni, J. J. (2008) Amino acid substitutions in homologs of the STAY-GREEN protein are responsible for the green-flesh and chlorophyll retainer mutations of tomato and pepper, Plant Physiol. 147, 179-87.

[20] Wei, Q., Guo, Y. & Kuai, B. (2011) Isolation and characterization of a chlorophyll degradation regulatory gene from tall fescue, Plant Cell Rep. 30, 1201-7.
[21] Zhou, C., Han, L., Pislariu, C., Nakashima, J., Fu, C., Jiang, Q., Quan, L., Blancaflor, E. B., Tang, Y., Bouton, J. H., Udvardi, M., Xia, G. & Wang, Z. Y. (2011) From model to crop: functional analysis of a STAY-GREEN gene in the model legume *Medicago truncatula* and effective use of the gene for alfalfa improvement, Plant Physiol. 157, 1483-96.
[22] Fang, C., Li, C., Li, W., Wang, Z., Zhou, Z., Shen, Y., Wu, M., Wu, Y., Li, G., Kong, L. A., Liu, C., Jackson, S. A. & Tian, Z. (2014) Concerted evolution of D1 and D2 to regulate chlorophyll degradation in soybean, Plant J. 77, 700-12.
[23] Sakuraba, Y., Schelbert, S., Park, S.-Y., Han, S.-H., Lee, B.-D., Andres, C. B., Kessler, F., Hörtensteiner, S. & Paek, N.-C. (2012) STAY-GREEN and chlorophyll catabolic enzymes interact at light-harvesting complex II for chlorophyll detoxification during leaf senescence in Arabidopsis, Plant Cell 24, 507-18.
[24] Sakuraba, Y., Kim, Y.-S., Yoo, S.-C., Hörtensteiner, S. & Paek, N.-C. (2013) 7-Hydroxymethyl chlorophyll a reductase functions in metabolic channeling of chlorophyll breakdown intermediates during leaf senescence, Biochem. Biophys. Res. Commun. 430, 32-7.
[25] Luo, Z., Zhang, J., Li, J., Yang, C., Wang, T., Ouyang, B., Li, H., Giovannoni, J. & Ye, Z. (2013) A STAY-GREEN protein SlSGR1 regulates lycopene and β-carotene accumulation by interacting directly with SlPSY1 during ripening processes in tomato, New Phytol. 198, 442-52.
[26] Mecey, C., Hauck, P., Trapp, M., Pumplin, N., Plovanich, A., Yao, J. & He, S. Y. (2011) A critical role of STAYGREEN/Mendel's I locus in controlling disease symptom development during *Pseudomonas syringae* pv tomato infection of Arabidopsis, Plant Physiol. 157, 1965-74.
[27] Sakuraba, Y., Lee, S.-H., Kim, Y.-S., Park, O. K., Hörtensteiner, S. & Paek, N.-C. (2014) Delayed degradation of chlorophylls and photosynthetic proteins in Arabidopsis autophagy mutants during stress-induced leaf yellowing, J. Exp. Bot. 65, 3915-3925.
[28] Sakuraba, Y., Park, S.-Y., Kim, Y.-S., Wang, S.-H., Yoo, S.-C., Hörtensteiner, S. & Paek, N.-C. (2014) Arabidopsis STAY-GREEN2 is a negative regulator of chlorophyll degradation during leaf senescence, Mol. Plant. 7, 1288-302.

[29] Rong, H., Tang, Y., Zhang, H., Wu, P., Chen, Y., Li, M., Wu, G. & Jiang, H. (2013) The Stay-Green Rice like (SGRL) gene regulates chlorophyll degradation in rice, J. Plant Physiol. 170, 1367-73.

[30] Earley, K. W., Haag, J. R., Pontes, O., Opper, K., Juehne, T., Song, K. & Pikaard, C. S. (2006) Gateway-compatible vectors for plant functional genomics and proteomics, Plant J. 45, 616-29.

[31] Zhang, X., Henriques, R., Lin, S. S., Niu, Q. W. & Chua, N. H. (2006) Agrobacterium-mediated transformation of *Arabidopsis thaliana* using the floral dip method, Nat. Protoc. 1, 641-6.

[32] Lichtenthaler, H.K. (1987) Chlorophylls and carotenoids: pigments of photosynthetic biomembranes, Methods Enzymol. 148, 350-82.

[33] Lim, P.-O., Kim, H.-J. & Nam, H.-G. (2007) Leaf senescence, Annu. Rev. Plant Biol. 58, 115-36.

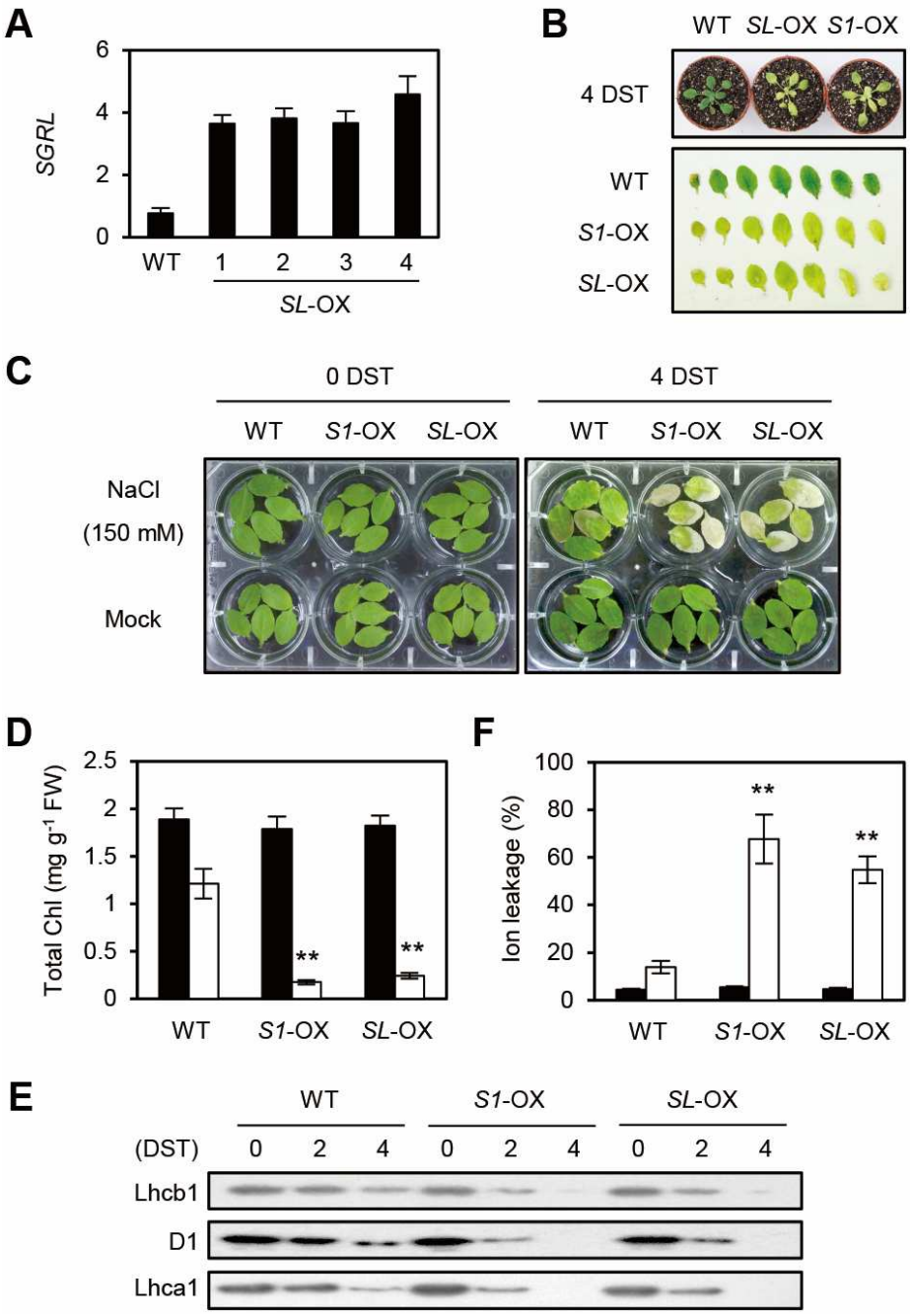

Fig. 1. The function of *Arabidopsis* SGRL in Chl degradation under salt stress.

(A) Expression levels of *SGRL* in transgenic lines containing *P35S:SGRL-GFP* (*SL*-OX). Total RNA was extracted from the rosette leaves of 3-week-old plants. By qRT-PCR, relative expression levels of *SGRL* were determined by normalizing to the transcript levels of *GAPDH* (glyceraldehyde phosphate dehydrogenase, At1g16300). Line #4, showing the highest expression of *SGRL-GFP* among 4 independent lines, was used in this study. WT, wild type. (B) Phenotype of WT, *SGR1*-OX (*P35S:SGR1-GFP*, *S1*-OX), and *SL*-OX plants at 4 days of salt treatment (200 mM NaCl). DST, day(s) of salt treatment. (C-F) Phenotypes (C),

total Chl levels (D), photosystem protein levels (E), and ion leakage rates (F) in WT, *S1*-OX, and *SL*-OX leaves before and after salt stress treatment (150 mM NaCl). (D, F) Black and white bars indicate 0 and 4 days of salt treatment (DST), respectively. Mean and SD were obtained from more than six samples. Asterisks indicate significant differences between WT and each OX line (Student's *t*-test *P*-values, $*P < 0.05$; $**P < 0.01$). (E) Antibodies against Lhcb1, Lhca1, and D1 were used for immunoblot analysis. These experiments were repeated at least three times with similar results.

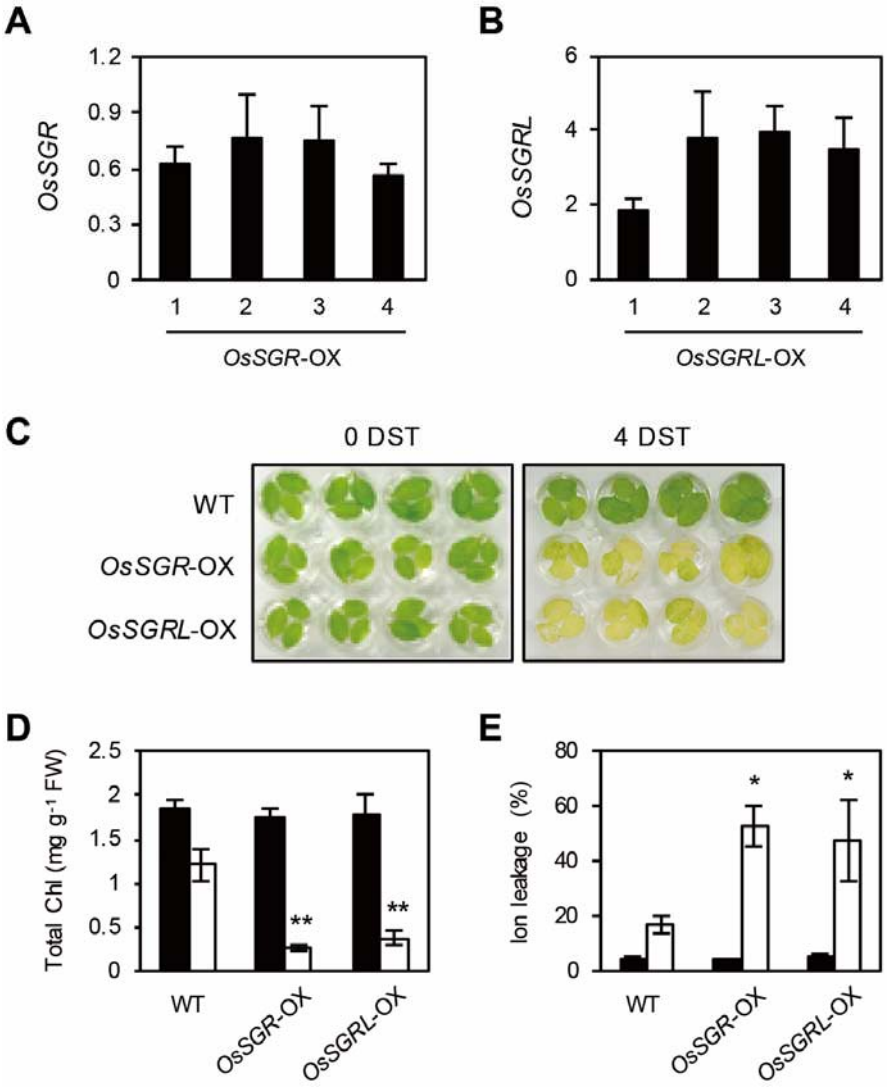

Fig. 2. Functional analysis of *OsSGR*-OX and *OsSGRL*-OX in *Arabidopsis* plants. (A, B) Expression levels of *OsSGR* (A) and *OsSGRL* (B) in the transgenic *Arabidopsis* lines containing *P35S:OsSGR-GFP* and *P35S:OsSGRL-GFP*. Total RNA was extracted from rosette leaves of 3-week-old plants. Using qRT-PCR, relative expression levels of *OsSGR* and *OsSGRL* were determined by normalizing to the transcript levels of *Arabidopsis GAPDH*. The *OsSGR*-OX (line #3) and *OsSGRL*-OX (line #3) plants were used in this study. Mean and SD were obtained from more than three samples. (C-E) Phenotypes (C), total Chl levels (D), and ion leakage rates (E) of detached leaves from 3-week-old WT, *OsSGR*-OX, and *OsSGRL*-OX plants under salt stress in continuous light. Black and white bars indicate 0 and 4 days of salt treatment (DST), respectively. Mean and SD were obtained from more than six samples. Asterisks indicate significant differences between WT and each OX line (Student's *t*-test *P*-values, $*P < 0.05$; $**P < 0.01$). These experiments were repeated at least three times with similar results.

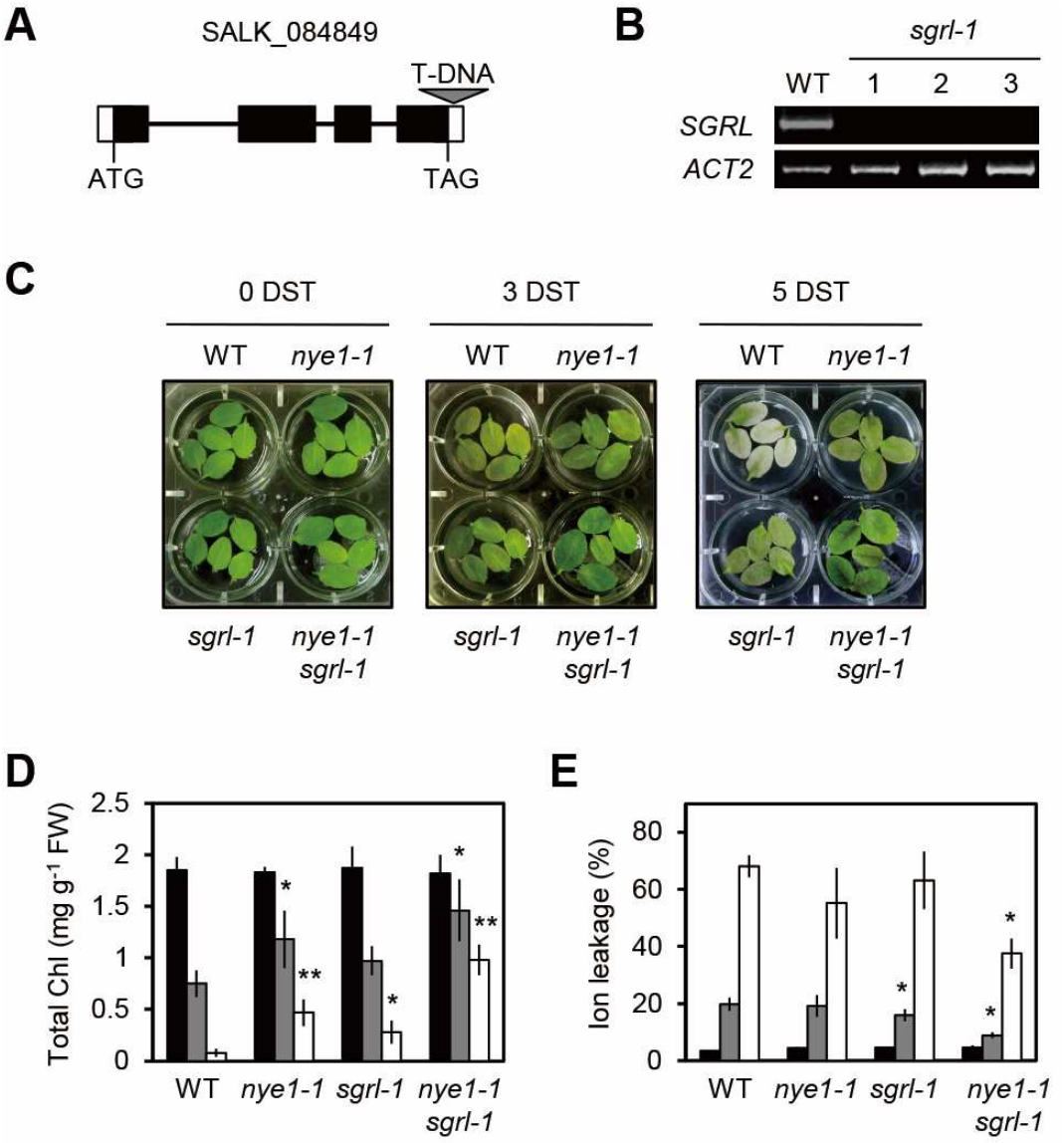

Fig. 3. Phenotypic characterization of single and double mutants in *SGRL* and *SGR1* under salt stress.

(A) Gene structure and T-DNA insertion in the 3' UTR of *SGRL* in the *Arabidopsis sgrl-1* mutant (SALK_084849). (B) Absence of *SGRL* transcripts in *sgrl-1* was confirmed by RT-PCR. *ACT2* (*ACTIN2*: At3g18780) was used as a loading control. The numbers of PCR cycles for the amplification of *SGRL* and *ACT2* transcripts were 30 and 25, respectively. Phenotypes (C), total Chl levels (D), and ion leakage rates (E) of detached leaves from 3-week-old WT, *nye1-1*, *sgrl-1*, and *nye1-1 sgrl-1* double mutants before (0 DST; black bars) and after 3 DST (grey bars) or 5 DST (white bars) with 150 mM NaCl. DST, days of salt treatment. Mean and SD were obtained from more than seven samples. Asterisks indicate significant difference between WT and each mutant (Student's *t*-test *P*-values, $*P < 0.05$; $**P < 0.01$). These experiments were repeated at least three times with similar results.

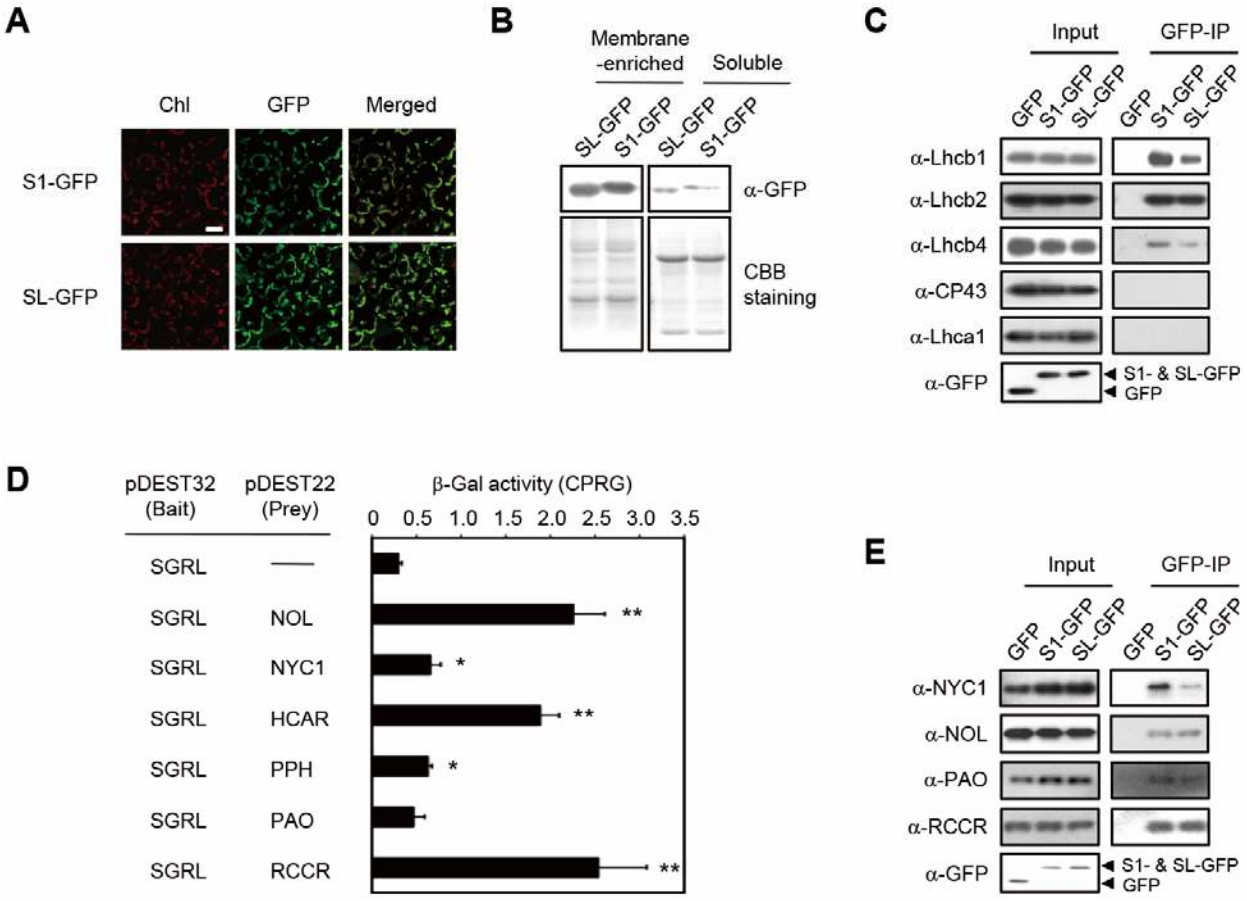

Fig. 4. Interaction of SGRL with LHCII and CCE proteins. (A) Chloroplast localization of SGRL-GFP (SL-GFP). SGR1-GFP (S1-GFP) was used as a positive control. Cotyledons of one-week-old seedlings were observed by confocal laser scanning microscopy. Bar = 50 μm. (B) SGRL-GFP proteins are more abundant in membrane-enriched protein fractions compared to soluble protein fractions (see Methods). Total protein extracts were obtained from the rosette leaves of 3-week-old plants. GFP fusion proteins were detected by immunoblotting with an anti-GFP antibody (upper panel). After immunoblot analysis, the blotted membranes were stained with Coomassie Brilliant Blue (CBB) as a loading control (lower panel). (C, E) SGRL interacts with LHCII subunits (C) and CCEs (E) *in vivo*. Three-week-old plants expressing SGR1-GFP (S1-GFP; positive control), SGRL-GFP (SL-GFP), and GFP (negative control) were incubated in darkness for 2 d. Membrane-enriched fractions were used for pull-down experiments using α-GFP antibody-conjugated agarose beads (GFP-IP). Co-precipitated proteins were detected by immunoblotting using respective antibodies. Input, immunoblot analysis of the fractions used for GFP-IP. (D) Interactions among SGRL and six CCEs in yeast two-hybrid assays. Relative β-galactosidase (β-Gal) activity was

determined in liquid assays using chlorophenol red-β-D-galactoside (CPRG) as substrate. An empty prey plasmid (-) was used as a negative control. Mean and SD values were obtained from five independent colonies. Asterisks indicate significant differences compared with the negative control (Student's *t*-test *P*-values, **P* < 0.05; ***P* < 0.01). These experiments were repeated at least three times with similar results.

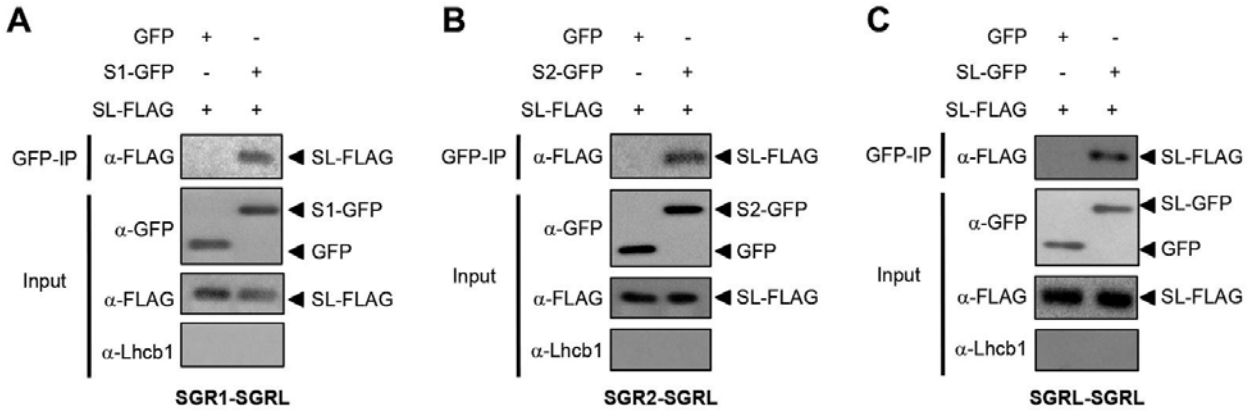

Fig. 5. Interactions of SGR1-SGRL, SGR2-SGRL, and SGRL-SGRL by *in vitro* pull-down assays.

Equal fresh weight of 1-week-old etiolated seedlings of transgenic *Arabidopsis* plants expressing GFP- or FLAG-tagged SGR proteins were co-homogenized. Each homogenate was used for *in vitro* pull-down assays with anti-GFP antibody (α-GFP)-conjugated agarose beads (GFP-IP), followed by immunoblot analysis using anti-FLAG antibody (α-FLAG). GFP transgenic plants (*P35S:GFP*) were used as a negative control. Etiolated seedlings did not accumulate LHCII proteins as confirmed by immunoblotting with α-Lhcb1. These experiments were repeated twice with similar results. S1, SGR1; S2, SGR2; SL, SGRL.

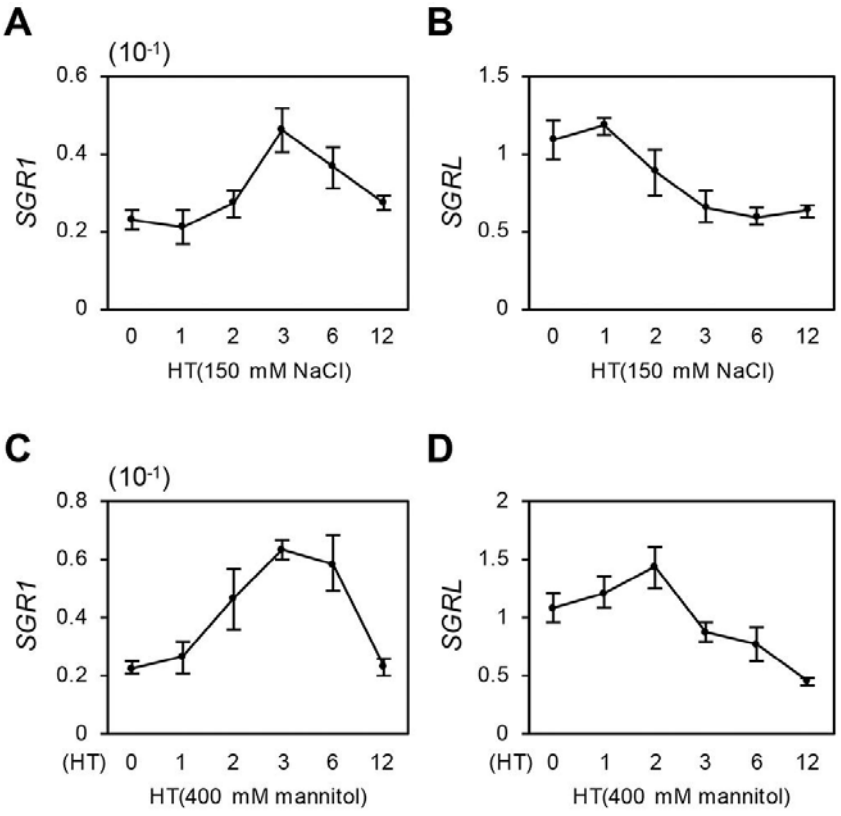

Fig. 6. Expression profiles of *SGR1* and *SGRL* under salt and osmotic stress. Expression levels of *SGR1* and *SGRL* were determined in the 2nd and 3rd rosette leaves of 3-week-old WT (Col-0) plants under salt stress (150 mM NaCl; A, B) or under osmotic stress (400 mM mannitol; C, D). By qRT-PCR, relative expression levels of *SGR1* (A and C) and *SGRL* (B and D) were determined by normalizing to the transcript levels of *GAPDH*. Mean and SD were obtained from more than three biological replicates. These experiments were repeated at least three times with similar results. HT, hours of treatment.